

# Discontinuity of the ultrafast electronic response of underdoped superconducting $\text{Bi}_2\text{Sr}_2\text{CaCu}_2\text{O}_{8+\delta}$ strongly excited by ultrashort light pulses

Claudio Giannetti,<sup>1,\*</sup> Giacomo Coslovich,<sup>2,3</sup> Federico Cilento,<sup>1</sup> Gabriele Ferrini,<sup>1</sup> Hiroshi Eisaki,<sup>4,5,†</sup> Nobuhisa Kaneko,<sup>5,‡</sup> Martin Greven,<sup>4,5</sup> and Fulvio Parmigiani<sup>2,6,§</sup>

<sup>1</sup>*Department of Physics, Università Cattolica del Sacro Cuore, Brescia I-25121, Italy*

<sup>2</sup>*Department of Physics, Università degli Studi di Trieste, Trieste I-34127, Italy*

<sup>3</sup>*Laboratorio Nazionale TASC, AREA Science Park, Basovizza Trieste I-34012, Italy*

<sup>4</sup>*Department of Applied Physics, Stanford University, Stanford, California 94305, USA*

<sup>5</sup>*Stanford Synchrotron Radiation Laboratory, Stanford, California 94305, USA*

<sup>6</sup>*Sincrotrone Trieste S.C.p.A., Basovizza I-34012, Italy*

(Received 5 December 2008; revised manuscript received 3 February 2009; published 3 June 2009)

We report the experimental evidence of an abrupt transition of the ultrafast electronic response of underdoped superconducting  $\text{Bi}_2\text{Sr}_2\text{CaCu}_2\text{O}_{8+\delta}$  under the impulsive photoinjection of a high density of excitations, using ultrashort laser pulses and avoiding significant laser heating. The direct proof of this process is the discontinuity of the transient optical electronic response, observed at a critical fluence of  $\Phi_{\text{th}} \approx 70 \mu\text{J}/\text{cm}^2$ . Below this threshold, the recovery dynamics is described by the Rothwarf-Taylor equations, whereas, above the critical intensity, a fast electronic response is superimposed to a slower dynamics related to the superconductivity recovery. We discuss our experimental findings within the frame of the available models for non-equilibrium superconductivity, i.e., the  $T_{\text{eff}}$  and  $\mu_{\text{eff}}$  models. The measured critical fluence is compatible with a first-order photoinduced phase transition triggered by the impulsive shift of the chemical potential. The measured value, significantly in excess of the condensation energy, indicates that, close to the threshold, the largest amount of energy is delivered to phonons or to other gap-energy excitations strongly coupled to Cooper pairs.

DOI: [10.1103/PhysRevB.79.224502](https://doi.org/10.1103/PhysRevB.79.224502)

PACS number(s): 74.40.+k, 74.72.Hs, 78.47.J-

## I. INTRODUCTION

The superconducting-to-normal state phase transition (SNPT) in high- $T_C$  superconductors (HTSC) is a poorly understood phenomenon.<sup>1</sup> So far, the superconducting (SC) phase formation in HTSC has been studied through optical techniques either at equilibrium in the frequency domain<sup>2</sup> or out of equilibrium in the time domain.<sup>3,4</sup> In particular, time-resolved optical spectroscopies have been widely applied to investigate the recovery dynamics of the equilibrium state in HTSC, excited by ultrashort laser pulses in the perturbative regime, i.e., when the density of photoinjected excitation is low and a small perturbation of the equilibrium excitation spectrum can be assumed. Most of the time-resolved experiments have been performed using high-repetition rate laser sources<sup>4</sup> to study the recombination dynamics of the photoinjected quasiparticles (QPs). The experimental findings evidenced a delicate interplay between electron-phonon and electron-electron interactions, usually modeled by the Rothwarf-Taylor coupled differential equations.<sup>5,6</sup>

Nonetheless, the average heating of the sample induced by the standard high-repetition rate laser sources<sup>4</sup> prevented scholars from investigating in detail the high-intensity pump regime, i.e., when the strong perturbation of the electronic distribution causes the closing of the superconducting gap. In this regime, a high-density  $n$  of excess QP is photoinjected, through an ultrashort pump pulse, modifying the equilibrium electron distribution on a timescale faster than the impulsively induced thermal heating. Under these conditions the free energy of the superconducting system  $F_{\text{SC}}(T, n)$  is varied along nonequilibrium pathways by the sudden modification

of  $n$ , whereas at equilibrium  $n(T, \mu \approx E_F)$  is univocally determined by the temperature and the chemical potential, through the Fermi-Dirac statistics.<sup>7</sup> Nonequilibrium superconductivity in the strong-excitation regime has been partially studied in BCS systems, without femtosecond time resolution, and evidenced the possibility of a nonthermal quenching of the superconducting phase, inducing a first-order phase transition to a metastable inhomogeneous state.<sup>8,9</sup>

Here we report time-resolved reflectivity measurements on underdoped  $\text{Bi}_2\text{Sr}_2\text{CaCu}_2\text{O}_{8+\delta}$  single crystals. By setting the proper repetition rate ( $< 100$  kHz) of the laser source we are able to impulsively excite the superconducting state obtaining a clear and unambiguous signature of a discontinuity of the electron dynamics at a critical fluence of  $\Phi_{\text{th}} \approx 70 \mu\text{J}/\text{cm}^2$ , while avoiding the sample average heating. In addition, we report the results of the numerical simulations of the dynamics of the SC gap closing and we show that at the measured threshold, the energy directly delivered to excitations far exceeds that required to photoinduce a nonthermal first-order SNPT, related to the impulsive shift of the chemical potential.

The possibility to impulsively modify the excitation spectrum of the superconducting condensate in HTSC, eventually quenching the SC phase, has widespread implications that will unlock the gate to a new physics and a new technology. (i) By photoinjecting a QP density in excess of a critical value, new metastable and inhomogeneous phases could be discovered.<sup>7-9</sup> (ii) From the intensity threshold necessary to induce the instability of the SC phase, the nature of the bosonic glue (if there is any<sup>10</sup>) necessary to form Cooper

pairs could be inferred. (iii) The measurement of the excitation and recovery dynamics constitutes a test for nonequilibrium models and sheds light on the timescale necessary for the definition of the thermodynamic properties of the system, such as the temperature and the chemical potential. (iv) The switching from a zero-resistance state to a finite-resistance state within a few hundred femtoseconds, and in the temperature range typical of HTSC, has evident implications for the development of optically controlled ultrafast electronics.

This work is organized as follows. In Sec. II we describe the experimental setup, and we show the time-resolved reflectivity measurements in the strong excitation regime. In Sec. III we discuss our findings within the frame of the only two available models for nonequilibrium superconductivity, i.e., the effective temperature ( $T_{\text{eff}}$ ) and chemical potential ( $\mu_{\text{eff}}$ ) models.<sup>11,12</sup> We report the results of the numerical simulations of the dynamics of the SC gap closing and we show that at the measured threshold, the energy directly delivered to the system far exceeds that required to photoinduce a nonthermal first-order SNPT, related to the impulsive shift of the chemical potential.

## II. EXPERIMENTAL RESULTS

### A. Setup

Time-resolved reflectivity measurements have been performed in the near infrared (IR) with a cavity-dumped Ti:sapphire oscillator producing 120 fs 1.5 eV light pulses. The output energy is  $\sim 50$  nJ/pulse at repetition rates tunable from 5.43 MHz to a single shot. By setting the proper repetition rate ( $\sim 100$  kHz), we are able to impulsively excite an underdoped  $\text{Bi}_2\text{Sr}_2\text{CaCu}_2\text{O}_{8+\delta}$  crystal ( $T_C=81$  K) with pump fluences ranging from 10 to  $850 \mu\text{J}/\text{cm}^2$ .

The value of  $T_C$  was measured through ac magnetic susceptibility, giving a transition amplitude of  $\pm 2$  K. The sample composition, homogeneity, and  $c$ -axis orientation dispersion were tested by means of x-ray diffraction both on bulk sample and on its powder. Results confirmed the absence of other structural phases of the compound and a lattice constant along the  $c$  axis of 3.09 nm with an angular dispersion of  $\Delta\Theta=1$ . The sample is anchored to a cold finger of a liquid-He open-cycle cryostat, through silver paste. The base pressure of the cryostat chamber is  $10^{-6}$  mbar. The condensation on the sample surface of water molecules, coming from the room temperature chamber walls, is avoided by protecting the sample through a transparent window.

### B. Results

#### 1. Normal state

Figure 1(a) shows the time-resolved reflectivity variation  $\Delta R/R(t)$  measured at room temperature. The impulsive variation, at zero delay, reflects the nonequilibrium excitation of the electronic system due to the pump pulses. In agreement with the literature,<sup>13,14</sup> the decay of the reflectivity in the normal state is well described by an extended two-temperature model.<sup>14</sup> Within this model, which is typical for metals, the fast dynamics of  $\sim 350$  fs is related to the electron-phonon relaxation. The inset of Fig. 1(a) displays

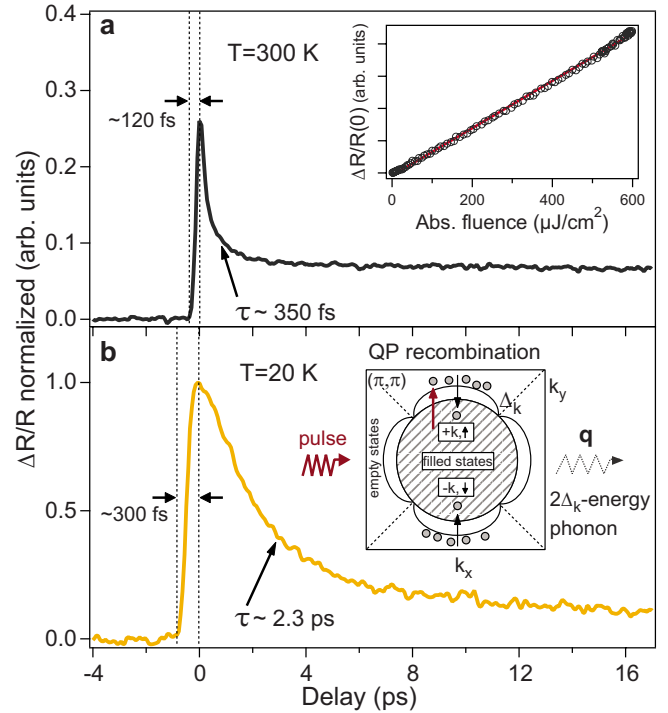


FIG. 1. (Color online) (a) Time-resolved reflectivity variation in underdoped  $\text{Bi}_2\text{Sr}_2\text{CaCu}_2\text{O}_{8+\delta}$  in the normal state ( $T=300$  K). The inset shows the  $\Delta R/R(t=0)$  scaling with the absorbed pump fluence in all the experimentally available intensity ranges. The solid line is a linear fit to the data. (b) Measured relaxation dynamics at  $T=20$  K. The measurement has been performed with  $\Phi_{\text{pump}} \approx 40 \mu\text{J}/\text{cm}^2$ , obtaining  $\Delta R/R(0) \approx 4 \times 10^{-4}$ . The inset shows a rough scheme of the excitation and relaxation processes of antinodal QP in the  $k$  space for a two-dimensional BCS-type superconductor with a spherical Fermi surface and a  $d$ -wave gap symmetry, with nodes in the  $(\pi, \pi)$  directions.

the maximum reflectivity variation  $\Delta R/R(t=0)$  as a function of the pump fluence. A linear dependence is observed over the entire experimentally available range.

#### 2. Superconducting state

The origin of the  $\Delta R/R$  variation measured in the superconducting state of cuprates has been extensively discussed in these last years.<sup>4,6,15-17</sup> The debate was focused on discriminating between an excited state absorption<sup>16</sup> and an anomalous spectral weight-shift mechanism.<sup>17</sup> While this problem is still open, a general agreement has been reached on the fact that the  $\Delta R/R$  variation in the near-IR/visible frequency range depends on the density of photoinjected quasiparticles.<sup>15,17</sup> This interpretation is so firmly established that transient reflectivity techniques are currently used to investigate the coexistence of superconducting-gap and pseudogap excitations in  $\text{Bi}_2\text{Sr}_2\text{CaCu}_2\text{O}_{8+\delta}$  on the base of the different recovery dynamics.<sup>18</sup> Accordingly, we will assume that the measured  $\Delta R/R$  signal below  $T_c$  is proportional to the density of the photoinjected QP. In Fig. 1(b) we report the  $\Delta R/R(t)$  signal measured at  $T=20$  K. When the sample is cooled below  $T_c$ , the maximum of the  $\Delta R/R$  signal is measured at  $t \approx 300$  fs and the decay time is on the order of

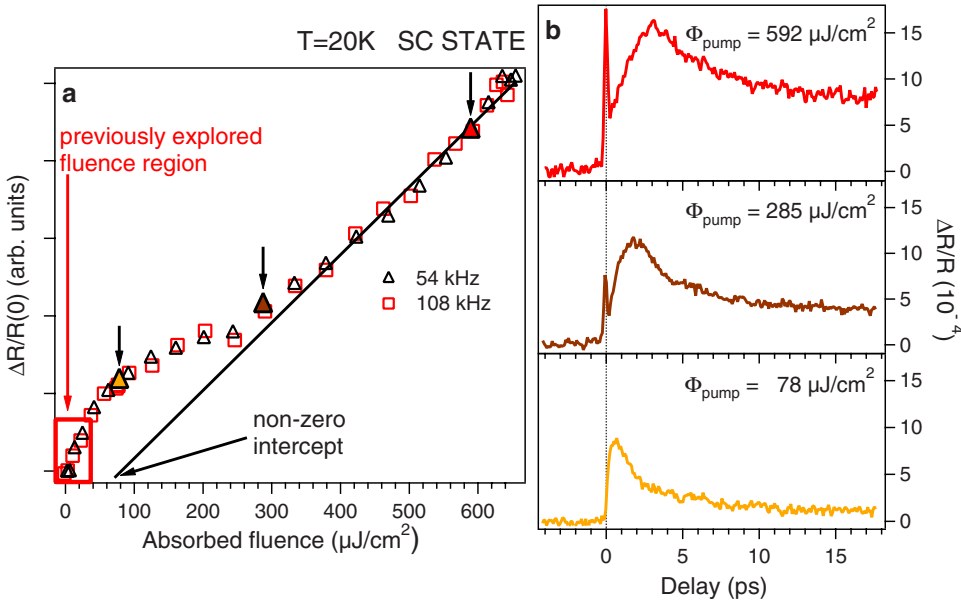


FIG. 2. (Color online) (a) Dependence of the transient reflectivity response at zero delay [ $\Delta R/R(t=0)$ ] on the absorbed excitation fluence in the superconducting state ( $T=20$  K). The linear fit at high-excitation levels (solid line) has a nonzero intercept. (b) Transient reflectivity dynamics at different absorbed fluences.

a few picoseconds, as shown in Fig. 1(b). The measured increase in the decay time in the SC phase is generally attributed to the suppression of the quasiparticle recombination process related to the opening of the superconducting gap<sup>6,19</sup> and, on the  $\mu\text{s}$  timescale, to the energy and momentum conservation rules of nodal QP (Ref. 20) [see inset of Fig. 1(b)]. As a consequence, the photoexcitation leads to the accumulation of a nonthermal distribution of QP on top of the SC gap at the antinodes, within  $\sim 1$  ps.

The dependence of  $\Delta R/R(t=0)$  in the SC phase ( $T=20$  K) on the pump intensity, at 108 kHz repetition rate, is reported in Fig. 2(a). The fluence range so far explored<sup>4</sup> with higher repetition rate sources, without significant local heating of the sample, is highlighted by the solid square. In this region we measured an increase in the signal, with a weak tendency to saturation.<sup>21</sup> Outside this region, we observed a progressive saturation of the signal up to the point at which a different linear behavior sets in. Note that the same behavior is observed at all the repetition rates lower than  $\sim 200$  kHz, as shown in Fig. 2(a). This is the experimental evidence that the observed transition is the effect of each individual pulse rather than the average effect of the train of pulses.

To interpret these results, we show in Fig. 2(b) the time-resolved reflectivity spectra at three different excitation fluences. At moderate absorbed fluences ( $\Phi_{\text{pump}}=78 \mu\text{J}/\text{cm}^2$ ) the dynamics is still similar to the low-intensity regime [Fig. 1(b)]. At larger absorbed energy densities ( $\Phi_{\text{pump}}=285 \mu\text{J}/\text{cm}^2$ )  $\Delta R/R(t)$  changes drastically; a fast peak appears, resembling the decay measured in the normal state, while the maximum of the reflectivity variation is shifted to  $\sim 2$  ps. At  $\Phi_{\text{pump}}=592 \mu\text{J}/\text{cm}^2$  the fast response overwhelms the slow component, as reflected by the linear behavior of the  $\Delta R/R(t=0)$  signal at high intensities, shown in Fig. 2(a). In this case, the slow  $\Delta R/R$  component exhibits a maximum at  $\sim 3$  ps, followed by a slower decay. In all the intensity regimes the slow dynamics is completed within  $\sim 15$  ps when a plateau proportional to the total absorbed fluence is recovered [see Fig. 3(a)]. The crucial observation is that the linear fit of the fast response at high-excitation

levels [fit in Fig. 2(a)] does not intercept the origin, suggesting that a minimum intensity ( $\Phi_{\text{th}}$ ) is necessary to activate this dynamics.

To confirm that the novel fast dynamics appears above this critical fluence  $\Phi_{\text{th}}$ , we show in Fig. 3(b) the femtosecond detail of the time-resolved reflectivity in the  $10\text{--}300 \mu\text{J}/\text{cm}^2$  fluence region. At low fluences the data can be perfectly fitted [red solid lines in Fig. 3(b)] with the numeric result of the integration of the Rothwarf-Taylor equations (RTEs),<sup>5</sup> describing the number  $n$  of excitations coupled to nonequilibrium gap-energy phonons (see the Appendix). The measured dynamics is very similar to other results reported in the literature at much lower excitation fluence ( $\Phi < 1 \mu\text{J}/\text{cm}^2$ ).<sup>4</sup> This is a direct evidence that in the low-intensity regime, the excitation spectrum and the SC gap are not destroyed in the probed area and they govern the recombination dynamics. The results of the fit indicate that the pump energy is mainly absorbed through phonon excitation. This finding satisfactorily explains that the decay dynamics is dominated by the inelastic scattering rate of high-energy phonons<sup>14</sup> without any intensity dependence<sup>4</sup> and that a constant delay of  $\sim 300$  fs of the maximum of signal is measured.<sup>6</sup> In this regime the  $\Delta R/R(t)$  signal scales linearly with the absorbed intensity. At absorbed energy densities larger than  $\sim 70 \mu\text{J}/\text{cm}^2$ , the data can no longer be fitted with the RTE and the dynamics abruptly changes. First, the fast peak emerges and increases rapidly. In Fig. 3(c) we show the weight of the fast peak, after the subtraction of the slow dynamics simulated by a coalescence model, as will be discussed in Sec. III B. At higher excitation intensities, not shown in Fig. 3(c), the weight of the fast component overwhelms the slow one and grows linearly with the pump intensity, as previously discussed. Second, the maximum of the slow component [circles in Fig. 3(b)] exhibits an abrupt plateau [Fig. 3(d)]. Third, the position of the maximum of the slow peak progressively shifts to higher delays [Fig. 3(e)]. To exclude disturbing effects connected to the average heating of the excited area, we numerically solved the heat equation and calculated the temperature increase profile on the

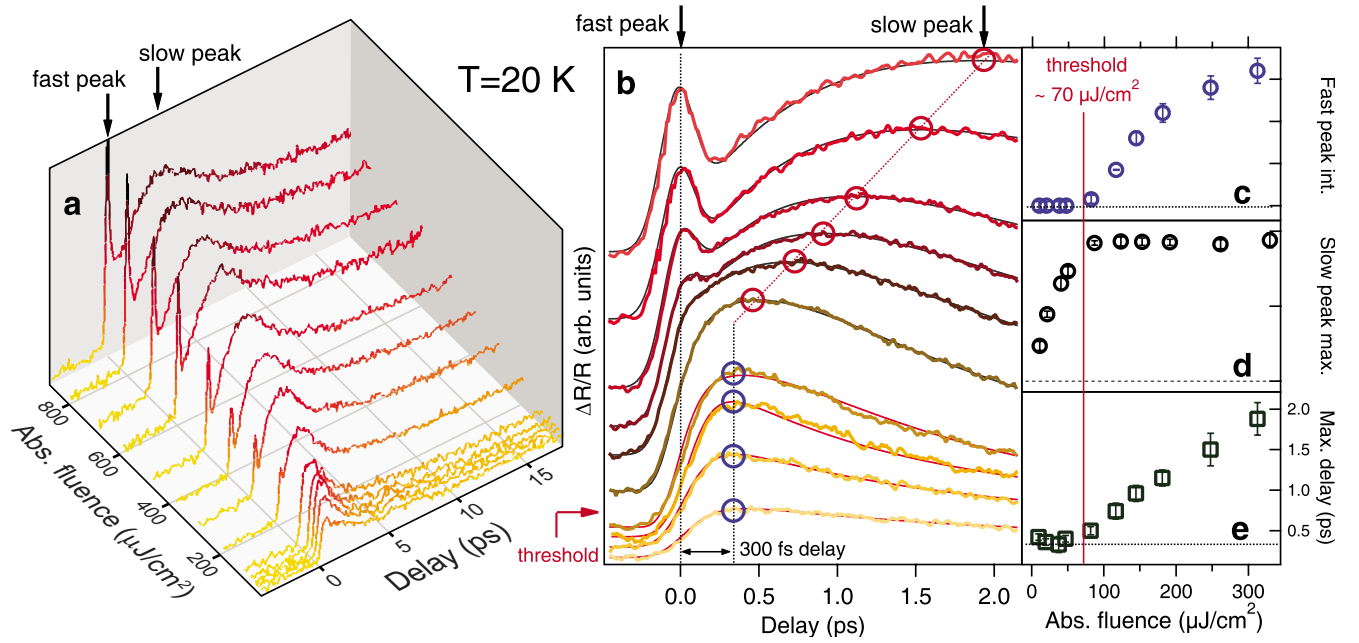


FIG. 3. (Color online) (a) Transient reflectivity traces as a function of both the time delay and the absorbed pump fluence (full experimental range). The measurements have been performed at  $T=20$  K and 108 kHz repetition rate. (b) Zoom of the region of interest for the energy threshold of the system. An offset proportional to the absorbed fluence is added for clarity (absorbed fluence varying from 9.4 to 313  $\mu\text{J}/\text{cm}^2$ ). Below  $\Phi_{\text{pump}} \sim 70$   $\mu\text{J}/\text{cm}^2$  the data are fitted with RTE (red solid lines). Above  $\Phi_{\text{th}}=70$   $\mu\text{J}/\text{cm}^2$  the product of the RTE solution and a coalescence dynamics (Ref. 22) is satisfactorily fitted to the data (black solid lines). (c) Intensity of the fast peak, after subtraction of the slow dynamics, as a function of the pump fluence. (d) Saturation of the slow component maximum above  $\Phi_{\text{th}}$ . (e) Position of the maximum of the  $\Delta R/R$  signal as the pump fluence is increased.

sample. The results indicate that at the threshold fluence, the maximum temperature increase is  $<10$  K.<sup>22</sup>

The unequivocal conclusion that the observed discontinuity of the  $\Delta R/R(t)$  dynamics at  $\Phi_{\text{pump}} > \Phi_{\text{th}}$  is the genuine signature of a transition of the electronic properties of the system comes from the following experimental evidences. (i) The femtosecond timescale of the fast peak confirms its electronic nature. Above  $\Phi_{\text{th}}$  this component abruptly appears and rapidly increases with the laser fluence. (ii) The measured nonzero intercept of this component (see Figs. 2 and 3) confirms that this result cannot be interpreted in terms of a saturating slow component related to the condensate dynamics and a fast one already present in low-intensity regime.<sup>23</sup> On the contrary, a minimum energy must be supplied to the system to observe the discontinuity of the dynamics reported here. Negative  $\Delta R/R$  components, possibly mimicking a nonzero intercept of the fast electronic dynamics, have never been measured on underdoped  $\text{Bi}_2\text{Sr}_2\text{CaCu}_2\text{O}_{8+\delta}$  below  $T_c$  at 1.55 eV photon energy.<sup>18,19</sup> (iii) The linear dependence of the “fast” peak on the absorbed fluence [see Figs. 2(a) and 3(a)] excludes any multiphoton process dominating the signal at high intensity. (iv) Coherent artifacts, possibly mimicking the fast dynamics at short delays, do not show any intensity threshold and must be excluded as the origin of our findings. (v) The discontinuity of the time-resolved dynamics is manifested not only in the emergence of the fast peak but also in the abrupt variation in the dynamics on the picosecond timescale, confirmed by the saturation and shift of the maximum of the slow  $\Delta R/R$  signal, as reported in Figs. 3(d) and 3(e).

### III. DISCUSSION

#### A. Nonequilibrium models

The intensity threshold measured in this work constitutes, in our opinion, a benchmark for the nonequilibrium superconductivity models applied to HTSC. In the standard approach to nonequilibrium superconductivity the SC gap and the excitation spectrum are assumed constant, and the recovery dynamics of the system is simply mimicked by the Rothwarf-Taylor rate equations<sup>6</sup> (see the Appendix). This approach is valid in the low-perturbation regime, but it is expected to fail when the modification of the excitation distribution is strong enough to modify the gap value and the excitation spectrum. Recent experiments of nonequilibrium terahertz conductivity of  $\text{Bi}_2\text{Sr}_2\text{CaCu}_2\text{O}_{8+\delta}$ ,<sup>24</sup> directly sensitive to the low-energy excitations, evidenced a reduction in the condensate fraction of about 85% upon excitation with 800 nm 12  $\mu\text{J}/\text{cm}^2$  pulses, whereas they did not evidence any significant variation in the decay dynamics, which is dependent on the gap value. These results suggest that, under this fluence regime, the induced strong perturbation of the excitation distribution is not sufficient to induce a complete collapse of the SC gap or a nonequilibrium transition to the normal state before the complete closing of the gap. On the contrary, we demonstrate a discontinuity in the dynamics on the femtosecond timescale at  $\sim 70$   $\mu\text{J}/\text{cm}^2$ , which represents the signature of the SC gap collapse. For this reason, the present results require a discussion within the frame of nonequilibrium models explicitly accounting for the change



of the excitation spectrum and gap value, as nonequilibrium excitations are photoinjected in the system.

In the BCS theory the dependence of the superconducting gap on the excitation distribution function is obtained through the gap equation

$$1 = N(0)U_{\text{pair}} \int_0^{\hbar\omega_D} \frac{d\epsilon_k}{\sqrt{\epsilon_k^2 + \Delta^2}} \tanh\left(\frac{\sqrt{\epsilon_k^2 + \Delta^2}}{2k_B T}\right), \quad (1)$$

where  $N(0)$  is the electronic density of states at the Fermi level,  $\Delta$  is the gap, and  $U_{\text{pair}}$  is the attractive pairing potential. In nonequilibrium superconductivity, the excess of excitations with respect to the thermal number ( $n_T$ ) is photoinjected by the pump pulse. The perturbation of the electron distribution can be mimicked both by introducing an effective temperature  $T_{\text{eff}}$  (Ref. 11) and an effective chemical potential  $\mu_{\text{eff}}$ .<sup>12</sup> Both the models predict a decrease in the superconducting gap  $\Delta(n_I, T)$  with the excitation density  $n_I$  [expressed in units of  $4N(0)\Delta(0,0)$ ], but with important differences.<sup>7</sup> In the  $T_{\text{eff}}$  model the gap dependence can be approximated by  $\Delta(n_I, 0)/\Delta(0,0) \approx 1 - 32(3n_I)^{3/2}/\pi^3$  and a complete closing is obtained at  $n_{\text{cr}}(T_{\text{eff}}) \approx 0.33$ , causing a second-order phase transition to the normal state. In the  $\mu_{\text{eff}}$  model, mimicking a shift of the excitation-distribution function decoupled from phonons, the gap closing is slower, i.e.,  $\Delta(n_I, 0)/\Delta(0,0) \approx 1 - 4\sqrt{2}n_I^{3/2}/3$ , and before the complete collapse of the gap at  $n_I \approx 0.65$ , the free energy of the superconducting state equals the normal state one. The free-energy difference between the two phases, in units of the condensation energy  $U_{\text{cond}} = N(0)\Delta^2(0)/2$ , is expressed<sup>7</sup> as  $\Delta F(n_I) \approx -1/2 + 16\sqrt{2}n_I^{3/2}/3$  and reduces to zero at  $n_{\text{cr}}(\mu_{\text{eff}}) \approx 0.16$ . The most important consequence is that, within the  $\mu_{\text{eff}}$  model, a first-order phase transition from the superconducting to the normal state can take place. We underline that the differences between the predictions of two models are not related to the density of excitation injected into the system but to their energy distribution.

To compare our results with the predictions of the  $T_{\text{eff}}$  model we performed the numeric integration of the gap Eq. (1) at the temperature  $T=20$  K and in the  $d$ -wave gap symmetry. The expected gap collapse is obtained at  $n_{\text{cr}}(T_{\text{eff}}) \approx 0.32$ , as shown in Fig. 4(a). To estimate the pump energy necessary to obtain this critical threshold we adopted the following strategy: the relation between the effective temperature and the excess QP number was calculated through the definition

$$n(T_{\text{eff}}) = \frac{1}{\Delta(0)} \left\langle \int_0^\infty [f(T_{\text{eff}}) - f(T)] d\epsilon_k \right\rangle, \quad (2)$$

where  $f(T_{\text{eff}})$  is the Fermi-Dirac distribution at temperature  $T_{\text{eff}}$  and  $\langle \dots \rangle$  indicates the average of the anisotropic  $d$ -wave gap over the  $k$  space. To calculate the different terms contributing to the energy absorption of the pump pulse as a function of  $T_{\text{eff}}$ , we considered, following Ref. 7, (i) the energy directly going in the quasiparticles ( $E_{\text{QP}}$ ) excitations,

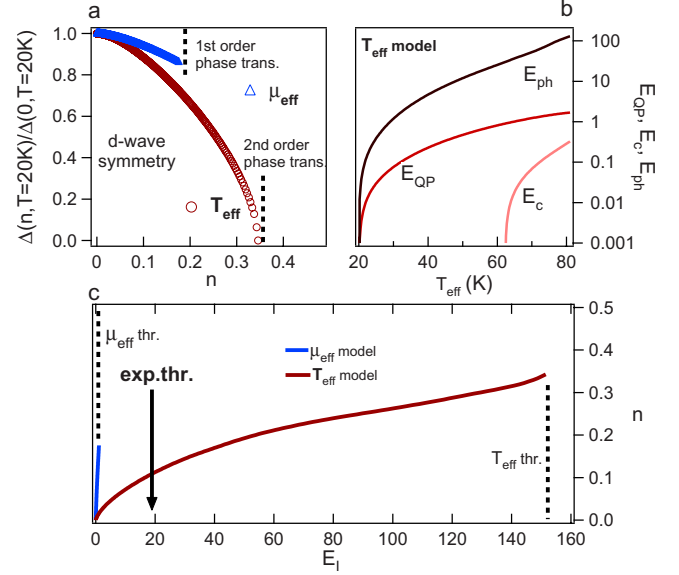


FIG. 4. (Color online) (a) Simulations of the gap closing within the  $T_{\text{eff}}$  and  $\mu_{\text{eff}}$  models ( $T=20$  K). (b) Different contributions to the energy variation as the effective temperature is varied. (c) Calculated excitation densities as a function of the absorbed energy.

$$E_{\text{QP}} = \frac{8}{\Delta^2(0)} \left\langle \int_0^\infty [E_k^{\text{eff}} f(T_{\text{eff}}) - E_k f(T)] d\epsilon_k \right\rangle, \quad (3)$$

where  $E_k^{\text{eff}} = \sqrt{\epsilon_k^2 + \Delta_k^2(T_{\text{eff}})}$ ; (ii) the variation in the energy of the superconducting condensate as a consequence of the excitations ( $E_c$ ),

$$E_c = \frac{4}{\Delta^2(0)} \left\langle \int_0^\infty E_k - E_k^{\text{eff}} + \frac{\Delta_k^2(T_{\text{eff}})}{2E_k^{\text{eff}}} [1 - 2f(T_{\text{eff}})] - \frac{\Delta_k^2(T)}{2E_k} [1 - 2f(T)] d\epsilon_k \right\rangle; \quad (4)$$

and (iii) the energy absorbed by the phonon system ( $E_{\text{ph}}$ ),

$$E_{\text{ph}} = \frac{1}{U_{\text{cond}}} \int_{2\Delta}^\infty \omega D(\omega) [p_{\text{BE}}(\omega, T_{\text{eff}}) - p_{\text{BE}}(\omega, T)], \quad (5)$$

where  $p_{\text{BE}}(\omega, T) = [\exp(\hbar\omega/k_B T) - 1]^{-1}$  and  $D(\omega)$  is the phonon density of states, taken from Ref. 25. The total absorbed energy, in units of the condensation energy, is simply given by  $E_I = E_{\text{QP}} + E_c + E_{\text{ph}}$ . In Fig. 4(b) we report the calculated contributions to  $E_I$  as a function of the effective temperature. At high pump fluences the energy absorbed by phonons is at least 1 order of magnitude larger than the other terms. The consequence is that the excess QP number photoinjected by the pump pulse is strongly suppressed by the phonon term and the gap collapse is obtained at very high pump fluences. We stress that a tendency toward saturation of the excitation density is predicted even below the intensity threshold necessary for a phase transition. As a consequence, the saturation in the optical properties, already reported in the literature,<sup>21,23,24</sup> is not in itself the signature of a phase transition or complete destruction of the SC phase.

At this point, the value considered for the condensation energy is crucial to compare the experimental intensity threshold to the numerical results. Calorimetric measurements are usually used to evaluate  $U_{\text{cond}} = \int_0^{T_C} T_C [S_N - S_{SC}] dT$ , where  $S_N$  and  $S_{SC}$  are the normal-state and superconducting-state entropies related to the electronic specific heat of the two phases.  $U_{\text{cond}} \sim 30$  J/mol has been measured for overdoped Bi2212,<sup>26</sup> whereas a decrease of about 1 order of magnitude was observed for underdoped samples exhibiting a pseudogap ( $U_{\text{cond}} \sim 3$  J/mol).<sup>26</sup> In this case, the measured condensation energy has to be interpreted as the energy difference between the superconducting-gap and pseudogap phases. For this reason we considered the value obtained for overdoped samples as the meaningful energy difference between the superconducting and the normal phases. Assuming  $U_{\text{cond}} \approx 30$  J/mol, we obtain that the total absorbed intensity necessary for the complete closing of the SC gap is  $E_I \approx 150$  [see Fig. 4(c)], at least seven times larger than the measured intensity threshold ( $E_{\text{th}} \approx 20$ ). We note that, considering a smaller value for the condensation energy, i.e.,  $U_{\text{cond}} \approx 3$  J/mol, the fraction of the pump energy absorbed by the phonons increases and the same discrepancy between the predicted and the measured threshold is obtained. These results allow us to exclude the complete closing of the superconducting gap, predicted by the  $T_{\text{eff}}$  model, as the cause of the measured discontinuity in the transient optical properties.

The accumulation of a nonthermal distribution of QP on the top of the SC gap can be accounted for by the  $\mu_{\text{eff}}$  model. In this model, the inclusion of the phonon contributions is not straightforward because the variation in the chemical potential describing the nonequilibrium distribution function does not affect the Bose-Einstein distribution  $p_{\text{BE}}(\omega, T)$  of the lattice excitations. Within the  $\mu_{\text{eff}}$  model, the absorbed energy is entirely provided to shift the chemical potential, and the predicted energy threshold is significantly smaller, i.e.,  $E_{\text{th}} \approx 2$ , as reported on Fig. 4(c). We conclude that, at the measured threshold, the energy delivered to the system is more than sufficient to photoinduce a first-order SNPT. The fact that the experimental threshold is larger than that predicted by the pure  $\mu_{\text{eff}}$  model can be ascribed to the energy absorption by phonons or by other excitations with energy larger than the SC gap.

We observe that while the  $T_{\text{eff}}$  and  $\mu_{\text{eff}}$  models have been designed for conventional superconductors, they can be extended, in principle, to any system, where a  $d$ -wave gap equation is valid and the free energy can be described in terms of the energy of excitations and of a superconducting condensate. In our opinion, the present work constitutes a first approach to address this question, nonetheless our results call for the development of more realistic nonequilibrium  $d$ -wave models, where both the shift of the chemical potential and the effective temperature of the QP are taken into account and the real band structure and density of states at the Fermi level are considered.

### B. Recovery dynamics

Under the assumption that the  $\Delta R/R(t)$  signal is proportional to the excitation density  $n$ , we should conclude that,

during the superconductivity recovery on the picosecond timescale,  $n$  increases, reaches a maximum, and decreases again (see Fig. 3). This is in contrast to the kinetics of the order parameter  $\eta$ , related to the average number of Cooper pairs, in a second-order phase transition,<sup>27</sup> described by the relaxation equation  $d\eta/dt = -2\gamma[(T - T_C)\alpha\eta + 2b\eta^3]$ , where  $\gamma$ ,  $\alpha$ , and  $b$  are positive coefficients. If the order parameter is impulsively decreased, the system monotonically recovers the equilibrium value  $\bar{\eta} = [\alpha(T_C - T)/2b]^{1/2}$  at  $T < T_C$ , i.e., the superconducting gap reconstruction implies a monotonic decrease in the excitations in the system, during a second-order phase transition. This consideration and the results of the simulations within the  $T_{\text{eff}}$  and  $\mu_{\text{eff}}$  models suggest that the measured discontinuity of the electronic dynamics is related to a phase transition with characteristics different from the thermal second-order one.

The scenario of a nonthermal first-order phase transition is further confirmed by fitting to the slow maximum a rough coalescence model.<sup>22,27</sup> We assume that within the first hundreds of femtoseconds, the free energy of the excited superconducting phase equals the free energy of the normal phase, leaving the system in an inhomogeneous mixture of the two phases. In the superconducting volume ( $q_{\text{SC}}$ ) the relaxation dynamics of  $n$  is slow and described by the RTE (see the Appendix), whereas in the normal fraction ( $1 - q_{\text{SC}}$ ) the decay of the excitations is extremely fast and is completed in a few hundreds of femtoseconds. On the picosecond timescale the metastable system can thus be schematized as superconducting regions surrounded by a normal volume, where the free energy of the superconducting phase is smaller than the free energy of the normal state and a coalescence process can start, in analogy with the case of a supersaturated solution. In this frame the detected  $\Delta R/R(t)$  signal is given by

$$\frac{\Delta R(t)}{R} \propto q_{\text{SC}}(t)n(t) + (1 - q_{\text{SC}})f_N(t), \quad (6)$$

where  $f_N(t)$  is the transient reflectivity signal related to the normal phase [see Fig. 1(a)]. We assume the dynamics of the superconducting fraction to be similar to the precipitation dynamics of the solute in a supersaturated solution, i.e.,  $q_{\text{SC}}(t) = 1 - [c/(t - t_0 + c)]$ , where  $c$  and  $t_0$  are coefficients related to the physical properties of the system and to the distribution of the grain size when the coalescence process begins.

In Fig. 3(b) we report the fit (black solid lines) of Eq. (6) to the measured dynamics in the high-intensity regime. On the picosecond timescale, the  $\Delta R(t)/R$  slow signal is dominated by the growth of the superconducting volume, resulting in the increase in the signal, whereas, on longer timescales the supersaturation tends to zero and the dynamics is regulated by the RTE. Within this model, the shift of the broad maximum [see Fig. 3(e)] is related to the increase in the time necessary to recover the SC phase at higher pump fluences.

### IV. CONCLUSIONS

In conclusion we demonstrated that the ultrafast electronic response of underdoped superconducting

$\text{Bi}_2\text{Sr}_2\text{CaCu}_2\text{O}_{8+\delta}$  exhibits a discontinuity at an excitation threshold of  $\Phi_{\text{th}} \approx 70 \mu\text{J}/\text{cm}^2$ . The results of the numerical simulations of the gap closing within the  $T_{\text{eff}}$  model allow us to rule out a quasithermal complete closing of the SC gap related to the increase in the effective temperature of the system. On the contrary, we calculated that, at the measured threshold, the energy delivered to the SC system far exceeds the energy necessary to induce a first-order nonthermal phase transition related to the shift of the chemical potential mimicking the nonthermal QP distribution within the first hundreds of femtoseconds. These results call for the development of a complete nonequilibrium model, taking into account both the shift of the chemical potential and the increase in the electronic effective temperature, to deal with the nonequilibrium “hot” QP distribution impulsively created by the laser pulses.

The possibility to photoinduce a first-order electronic phase transition in a superconducting HTSC system opens intriguing possibilities. First, the present measurements underline the interesting question of the real nature of the metastable final state after the photoexcitation of a SNPT and its relationship with the underlying pseudogap state, where the  $\Delta R/R(t)$  dynamics drastically changes.<sup>18</sup> The detailed investigation of the electronic dynamics of the final state should help in discriminating between a pseudogap phase competing and coexisting with the superconducting phase. Second, a weak first-order SNPT is expected at  $|T - T_C|/T_C \approx 10^{-6}$  K because of the effects of the order parameter fluctuations.<sup>28</sup> Upon impulsive excitation, the first-order phase transition could be photoinduced by the sudden variation in the order parameter, where the thermodynamic temperature  $T \ll T_C$  is fixed. This possibility opens the way to the study of new dynamical phases of nonequilibrium condensed-matter systems. Third, the rough coalescence model satisfactorily fits the data even at very high fluences, where  $t_0 > 0$ , i.e., the SC phase is completely destroyed and the coalescence begins at positive delays. The lack of a signature of an earlier nucleation process could suggest a role played by the intrinsic inhomogeneity of the SC ground state at the nanometric scale.<sup>29</sup> Fourth, a further investigation of the velocity of the first-order photoinduced SNPT can have important consequences on the understanding of the binding mechanism<sup>1</sup> to form Cooper pairs in HTSC. The presence of a bottleneck in the timescale of the SNPT could be the fingerprint of the coupling mechanism.

## ACKNOWLEDGMENTS

This work was supported by the MIUR under the Contract No. FIRB-RBNE0155X7. The crystal growth work at Stanford University was supported by DOE under Contracts No. DE-FG03-99ER45773 and No. DE-AC03-76SF00515 and by NSF under Grant No. DMR9985067.

## APPENDIX: ROTHWARF-TAYLOR EQUATIONS

The nonequilibrium dynamics in superconductors is usually successfully interpreted<sup>6,19</sup> within the phenomenological frame of the Rothwarf-Taylor equations (RTE),<sup>5</sup>

$$\dot{n} = I_{\text{QP}}(t) + 2\gamma p - \beta n^2, \quad (\text{A1})$$

$$\dot{p} = I_{\text{ph}}(t) - \gamma p + \beta n^2/2 - \gamma_{\text{esc}}(p - p_T), \quad (\text{A2})$$

describing the density of excitations  $n$  coupled to phonons and  $p$  being the gap-energy phonon density. The nonequilibrium QP and phonons are photoinjected in the system through the  $I_{\text{QP}}(t)$  and  $I_{\text{ph}}(t)$  terms. A Gaussian temporal profile of  $I_{\text{QP}}(t)$  and  $I_{\text{ph}}(t)$ , with the same time width as the laser pulse, is assumed. The coupling of the electronic and phonon population is obtained through (a) the annihilation of a Cooper pair via gap phonon absorption ( $p\gamma$  term) and (b) the emission of gap phonons during the two-body direct recombination of excitations to form a Cooper pair ( $\beta n^2$  term). In the phonon bottleneck regime ( $\gamma > \gamma_{\text{esc}}$ ) the excitation relaxation is ultimately regulated by the escape rate of the nonequilibrium gap-energy phonons [ $\gamma_{\text{esc}}(p - p_T)$  term, where  $p_T$  is the thermal phonon density]. The  $\gamma_{\text{esc}}$  value is determined both by the escape rate of the nonequilibrium phonons from the probed region and by the energy relaxation through inelastic scattering with the thermal phonons. Below  $\Phi_{\text{th}}$ , the measured QP dynamics, reported in Figs. 1(b) and 3(b), is satisfactorily reproduced by considering only the  $I_{\text{ph}}(t)$  term, i.e., assuming that the pump energy is mainly absorbed through excitation of the phonon population. This result is in agreement with both theoretical predictions within the  $T_{\text{eff}}$  model<sup>7</sup> and experimental observations on YBCO (Refs. 30 and 31) and  $\text{MgB}_2$ .<sup>32</sup> In the fitting procedure we assumed  $\beta \approx 0.1 \text{ cm}^2/\text{s}$ , as reported in the literature.<sup>19</sup> The determined free parameters are  $\gamma p(t=0) \approx 10^{14} \text{ ps}^{-1} \text{ cm}^{-2}$  and  $\gamma_{\text{esc}} = (1.5 \pm 0.1) \text{ ps}^{-1}$ . These values are compatible with both the results obtained on LSCO (Ref. 33) and the theoretical estimations of anharmonic processes in YBCO.<sup>3</sup>

\*c.giannetti@dmf.unicatt.it

<sup>†</sup>Present address: Nanoelectronics Research Institute, National Institute of Advanced Industrial Science and Technology, Tsukuba, Ibaraki 305-8568, Japan.

<sup>‡</sup>Present address: National Metrology Institute of Japan, National Institute of Advanced Industrial Science and Technology, Tsukuba, Ibaraki 305-8568, Japan.

<sup>§</sup>fulvio.parmigiani@elettra.trieste.it

<sup>1</sup>P. Monthoux, D. Pines, and G. G. Lonzarich, Nature (London)

**450**, 1177 (2007).

<sup>2</sup>D. N. Basov and T. Timusk, Rev. Mod. Phys. **77**, 721 (2005).

<sup>3</sup>V. V. Kabanov, J. Demsar, B. Podobnik, and D. Mihailovic, Phys. Rev. B **59**, 1497 (1999).

<sup>4</sup>N. Gedik, M. Langner, J. Orenstein, S. Ono, Y. Abe, and Y. Ando, Phys. Rev. Lett. **95**, 117005 (2005).

<sup>5</sup>A. Rothwarf and B. N. Taylor, Phys. Rev. Lett. **19**, 27 (1967).

<sup>6</sup>V. V. Kabanov, J. Demsar, and D. Mihailovic, Phys. Rev. Lett. **95**, 147002 (2005).

- <sup>7</sup>E. J. Nicol and J. P. Carbotte, *Phys. Rev. B* **67**, 214506 (2003).
- <sup>8</sup>L. R. Testardi, *Phys. Rev. B* **4**, 2189 (1971).
- <sup>9</sup>R. Sobolewski, D. P. Butler, T. Y. Hsiang, C. V. Stancampiano, and G. A. Mourou, *Phys. Rev. B* **33**, 4604 (1986).
- <sup>10</sup>P. W. Anderson, *Science* **316**, 1705 (2007).
- <sup>11</sup>W. H. Parker, *Phys. Rev. B* **12**, 3667 (1975).
- <sup>12</sup>C. S. Owen and D. J. Scalapino, *Phys. Rev. Lett.* **28**, 1559 (1972).
- <sup>13</sup>S. D. Brorson, A. Kazeroonian, D. W. Face, T. K. Cheng, G. L. Doll, M. S. Dresselhaus, G. Dresselhaus, E. P. Ippen, T. Venkatesan, X. D. Wu, and A. Inam, *Solid State Commun.* **74**, 1305 (1990).
- <sup>14</sup>L. Perfetti, P. A. Loukakos, M. Lisowski, U. Bovensiepen, H. Eisaki, and M. Wolf, *Phys. Rev. Lett.* **99**, 197001 (2007).
- <sup>15</sup>D. Dvorsek, V. V. Kabanov, J. Demsar, S. M. Kazakov, J. Karpinski, and D. Mihailovic, *Phys. Rev. B* **66**, 020510(R) (2002).
- <sup>16</sup>J. Demsar, R. D. Averitt, V. V. Kabanov, and D. Mihailovic, *Phys. Rev. Lett.* **91**, 169701 (2003).
- <sup>17</sup>N. Gedik, J. Orenstein, R. Liang, D. A. Bonn, and W. N. Hardy, *Phys. Rev. Lett.* **91**, 169702 (2003).
- <sup>18</sup>Y. H. Liu, Y. Toda, K. Shimatake, N. Momono, M. Oda, and M. Ido, *Phys. Rev. Lett.* **101**, 137003 (2008).
- <sup>19</sup>N. Gedik, P. Blake, R. C. Spitzer, J. Orenstein, R. Liang, D. A. Bonn, and W. N. Hardy, *Phys. Rev. B* **70**, 014504 (2004).
- <sup>20</sup>B. J. Feenstra, J. Schutzmann, D. van der Marel, R. Perez Pina, and M. Decroux, *Phys. Rev. Lett.* **79**, 4890 (1997).
- <sup>21</sup>G. P. Segre, N. Gedik, J. Orenstein, D. A. Bonn, R. Liang, and W. N. Hardy, *Phys. Rev. Lett.* **88**, 137001 (2002).
- <sup>22</sup>For further details, see C. Giannetti, G. Coslovich, F. Cilento, G. Ferrini, H. Eisaki, N. Kaneko, M. Greven, and F. Parmigiani, arXiv:0804.4822 (unpublished).
- <sup>23</sup>R. A. Kaindl, M. Woerner, T. Elsaesser, D. C. Smith, J. F. Ryan, G. A. Farnan, M. P. McCurry, and D. G. Walmsley, *Physica C* **341–348**, 2213 (2000).
- <sup>24</sup>M. A. Carnahan, R. A. Kaindl, J. Orenstein, D. S. Chemla, S. Oh, and J. Eckstein, *Physica C* **408–410**, 729 (2004).
- <sup>25</sup>D. Shimada, N. Tsuda, U. Paltzer, and F. W. de Wette, *Physica C* **298**, 195 (1998).
- <sup>26</sup>J. W. Loram, J. L. Luo, J. R. Cooper, W. Y. Liang, and J. L. Tallon, *Physica C* **341–348**, 831 (2000).
- <sup>27</sup>E. M. Lifshitz and L. P. Pitaevskii, *Physical Kinetics* (Butterworth-Heinemann, Oxford, 1981).
- <sup>28</sup>B. Halperin, T. Lubensky, and S. K. Ma, *Phys. Rev. Lett.* **32**, 292 (1974).
- <sup>29</sup>K. McElroy, R. W. Simmonds, J. E. Hoffman, D. H. Lee, J. Orenstein, H. Eisaki, S. Uchida, and J. C. Davis, *Nature (London)* **422**, 592 (2003).
- <sup>30</sup>S. G. Han, Z. V. Vardeny, K. S. Wong, O. G. Symko, and G. Koren, *Phys. Rev. Lett.* **65**, 2708 (1990).
- <sup>31</sup>A. Frenkel, *Phys. Rev. B* **48**, 9717 (1993).
- <sup>32</sup>J. Demsar, R. D. Averitt, A. J. Taylor, V. V. Kabanov, W. N. Kang, H. J. Kim, E. M. Choi, and S. I. Lee, *Phys. Rev. Lett.* **91**, 267002 (2003).
- <sup>33</sup>P. Kusar, V. V. Kabanov, S. Sugai, J. Demsar, T. Mertelj, and D. Mihailovic, *Phys. Rev. Lett.* **101**, 227001 (2008).